



Published in final edited form as:

J Control Release. 2015 June 10; 207: 7–17. doi:10.1016/j.jconrel.2015.03.034.

Sequential delivery of angiogenic growth factors improves revascularization and heart function after myocardial infarction

Hassan K. Awada^a, Noah R. Johnson^a, and Yadong Wang^{a,b,c,d,*}

^aDepartment of Bioengineering and the McGowan Institute for Regenerative Medicine, University of Pittsburgh, Pittsburgh, PA 15219, USA

^bDepartment of Chemical and Petroleum Engineering, University of Pittsburgh, Pittsburgh, PA 15219, USA

^cDepartment of Surgery, University of Pittsburgh, Pittsburgh, PA 15219, USA

^dDepartment of Mechanical Engineering and Materials Science, University of Pittsburgh, Pittsburgh, PA 15219, USA

Abstract

Treatment of ischemia through therapeutic angiogenesis faces significant challenges. Growth factor (GF)-based therapies can be more effective when concerns such as GF spatiotemporal presentation, bioactivity, bioavailability, and localization are addressed. During angiogenesis, vascular endothelial GF (VEGF) is required early to initiate neovessel formation while platelet-derived GF (PDGF-BB) is needed later to stabilize the neovessels. The spatiotemporal delivery of multiple bioactive GFs involved in angiogenesis, in a close mimic to physiological cues, holds great potential to treat ischemic diseases. To achieve sequential release of VEGF and PDGF, we embed VEGF in fibrin gel and PDGF in a heparin-based coacervate that is distributed in the same fibrin gel. *In vitro*, we show the benefits of this controlled delivery approach on cell proliferation, chemotaxis, and capillary formation. A rat myocardial infarction (MI) model demonstrated the effectiveness of this delivery system in improving cardiac function, ventricular wall thickness, angiogenesis, cardiac muscle survival, and reducing fibrosis and inflammation in the infarct zone compared to saline, empty vehicle, and free GFs. Collectively, our results show that this delivery approach mitigated the injury caused by MI and may serve as a new therapy to treat ischemic hearts pending further examination.

Keywords

Therapeutic angiogenesis; Myocardial infarction; Controlled release; Coacervate; Fibrin gel; Growth factors

© 2015 Published by Elsevier B.V.

*Corresponding author at: Department of Bioengineering, University of Pittsburgh, Pittsburgh, PA 15261, USA. Tel.: +1 412 624 7196; fax: +1 412 624 3699., yaw20@pitt.edu (Y. Wang).

Publisher's Disclaimer: This is a PDF file of an unedited manuscript that has been accepted for publication. As a service to our customers we are providing this early version of the manuscript. The manuscript will undergo copyediting, typesetting, and review of the resulting proof before it is published in its final citable form. Please note that during the production process errors may be discovered which could affect the content, and all legal disclaimers that apply to the journal pertain.

1. Introduction

Ischemic heart disease is a leading cause of morbidity and mortality in the United States. In 2010, the estimated direct and indirect cost of heart disease was approximately \$200 billion. In that year, myocardial infarction (MI) was prevalent in 7.6 million Americans.

Approximately, 15% of the people who experience a heart attack (MI) in a given year will die of it [1]. During MI, insufficient blood supply to a region of the heart muscle (infarct zone) leads to cell death and pathological remodeling which often progresses to heart failure over time [2]. Therapeutic angiogenesis aims to restore blood flow to the affected ischemic heart muscles by new blood vessel formation from existing vasculature [3–5].

Revascularization by pro-angiogenic therapies has thus far failed to provide satisfactory outcomes in clinical trials [6–8]. Bolus injections of single GFs led to limited efficacy because of loss of bioactivity, missing critical signals in the cascade of events that lead to stable angiogenesis, among others. An effective angiogenesis-based therapy can be developed when a comprehensive understanding of angiogenic mechanisms becomes available [8, 9]. Repair and regeneration strategies should focus on utilizing the growth factors (GFs) that play vital roles in the process of angiogenesis, as well as the need to administer them spatiotemporally and in bioactive conformations [6, 7, 10–12].

Many studies have shown that GFs such as fibroblast growth factor-2 (FGF-2), vascular endothelial growth factor (VEGF), angiopoietin-2 (Ang-2) are key factors in triggering angiogenesis, but these factors alone may result in leaky and immature blood vessels that are susceptible to early regression [13, 14]. Other GFs such as platelet-derived growth factor (PDGF) and angiopoietin-1 (Ang-1) help stabilize neovessels [15, 16]. Among potential angiogenic candidates, VEGF and PDGF are promising due to their potency, specificity, and cardioprotective roles [5, 6, 17, 18]. VEGF, an endothelial-specific factor, triggers the process through endothelial cell (EC) sprouting, proliferation, migration, and lumen formation, and is thus primarily needed in the first few days of angiogenesis [17, 19, 20]. After luminal formation, mural cells are recruited by PDGF to cover the neovessels and provide stabilization; therefore PDGF is required at a later stage of angiogenesis to prevent vessel regression or the formation of aberrant and leaky vessels [15, 17]. It has been shown that early-stage angiogenic factors can have antagonistic effects on late-stage factors and vice versa, when present simultaneously [21–23]. Therefore, it appears imperative to sequentially administer these two GFs to imitate their physiological presence during angiogenesis.

To control the spatiotemporal cues and protect the bioactivity of VEGF and PDGF, we developed a controlled delivery system composed of fibrin gel and a recently developed biocompatible heparin-based coacervate that we characterized in previous reports [24, 25]. Fibrin gel, formed through the polymerization of fibrinogen by thrombin, is commercially available and has been used for protein and cell delivery [26]. Complex coacervates are formed by mixing oppositely charged polyelectrolytes resulting in spherical droplets of organic molecules held together noncovalently and apart from the surrounding liquid and have shown potential in sustained protein delivery [24, 25, 27–34]. VEGF was embedded into the fibrin gel, while PDGF was loaded into the coacervate then embedded into the gel. The coacervate was used to control the release of PDGF based on its affinity to heparin. This

system provided rapid release of VEGF followed by slow and sustained release of PDGF from a single injection. Here we report the effects of sequentially delivered VEGF and PDGF on revascularization and heart function after MI in rats.

2. Materials and methods

2.1. Release kinetics assay

The release assay (n=3) was performed using 100 ng of VEGF₁₆₅ and 100 ng of PDGF-BB (PeproTech, Rocky Hill, NJ). PDGF Coacervate was made by mixing PDGF with heparin first (Scientific Protein Labs, Waunakee, WI), then with the polycation, poly(ethylene arginyl aspartate diglyceride) (PEAD) [27] at PEAD:heparin:GF mass ratio of 50:10:1. Fibrin gel was made by mixing 90 μ l of 20 mg/ml fibrinogen solution (Sigma-Aldrich, St. Louis, MO) containing unbound VEGF and the PDGF coacervate with 5 μ l of 1 mg/ml thrombin solution (Sigma-Aldrich, St. Louis, MO) and 5 μ l of 1 mg/ml aprotonin solution (Sigma-Aldrich, St. Louis, MO). A 100 μ l of 0.9% saline was deposited on top of fibrin gel to be collected at 1 hr, 16 hrs, 1, 4, 7, 14, and 21 days. The samples were incubated at 37°C. After centrifugation at 12,100 g for 10 min, supernatant was aspirated and stored at -80°C to detect amount of released GFs by ELISA kits (PeproTech, Rocky Hill, NJ). The absorbance at 450/540 nm was measured by a SynergyMX plate reader (Biotek, Winooski, VT). Normalizing standards (n=3) were prepared using the same amounts of free GFs in 100 μ l of 0.9% saline.

2.2. Smooth muscle cell chemotaxis assay

Chemotactic media was prepared as 500 μ l MCDB-131+10% fetal bovine serum (FBS) per well in a 24-well plate with group-specific addition of saline (basal media), empty vehicle, or 100 ng free PDGF or in the coacervate. 8 μ m pore size culture inserts (BD Falcon, Franklin Lakes, NJ) were placed in each well and 10⁴ baboon smooth muscle cells (SMCs) were pipetted into the insert in 200 μ l basal media and plate was incubated at 37°C. After 12 hrs, cells remaining inside the insert were removed from the upper surface of the membrane with a cotton swab. Cells that had migrated to the lower surface of the membrane were then fixed in methanol for 15 min. Cells were incubated for 15 min in the dark with PicoGreen fluorescent dye from Quant-iT PicoGreen dsDNA Kit (Molecular Probes, Eugene, OR), diluted 200-fold to working concentration in DPBS. Cells were imaged with a fluorescent microscope (Eclipse Ti; Nikon, Tokyo, Japan) and images were taken in the center of each well in three wells per group and counted manually.

2.3. Endothelial and smooth muscle cells proliferation assays

Human umbilical vein endothelial cells (HUVEC) (ATCC, Manassas, VA) or baboon SMCs were seeded at 10⁴ cells per well in a 96-well plate and cultured in EGM-2 media (Lonza, Walkersville, MD) and MCDB131+0.2% FBS media, respectively. Group-specific additions were made to media with GF concentrations at 20 ng/ml per well for SMCs and 25 ng/ml of each GF per well for HUVEC. The plates were incubated for 48 hrs at 37°C. 20 μ l of pre-prepared BrdU label was then added for 4 hrs and the proliferation assays were performed according to kit's instructions (Millipore, Temecula, CA). The absorbance at 450/540 nm

was measured by a SynergyMX plate reader. Absorbance proliferation values were normalized to basal media value.

2.4. Ex vivo rat aortic ring assay

Thoracic rat aortae (n=3 per group) were dissected according to established protocols [35, 36], cleaned from fibro-adipose tissue, and cut into approximately 1.5 mm ring segments. Rings were serum-starved overnight in serum-free endothelial basal medium (EBM). Next day, the rings were embedded in the center of a 3D fibrin matrix that contained different treatment groups (GF dose of 250 ng) with luminal axis perpendicular to the bottom of the well in a 24-well plate. 500 μ L of EBM was placed on top of gel. Rings were incubated at 37°C for 6 days. Rings were then imaged using brightfield (BF) microscopy and quantified in terms of microvasculature sprouting area in 3 wells per group.

2.5. Rat acute myocardial infarction model

University of Pittsburgh Institutional Animal Care and Use Committee (IACUC) approval was obtained prior to beginning all animal studies. MI and injections were performed as previously described [37]. Briefly, 6–7 week old male Sprague-Dawley rats (Charles River Labs, Wilmington, MA) were anesthetized with isoflurane (Butler Schein, Dublin, OH), intubated, and connected to a mechanical ventilator. The ventral side was shaved and a small incision was made through the skin. The muscle and ribs above heart were separated. The heart was exposed and MI was induced by ligation of the left anterior descending (LAD) coronary artery using a 6-0 polypropylene suture (Ethicon, Bridgewater, NJ). Five minutes after the induction of MI, 100 μ l of saline, empty vehicle, free VEGF+PDGF (1.5 μ g of each GF), or sequentially delivered VEGF+PDGF (using fibrin gel-coacervate system) solutions were injected intramyocardially at 3 equidistant points around the infarct zone using a 31 G needle (BD, Franklin Lakes, NJ). For injections of fibrin gel, thrombin was added to fibrinogen solution and injected shortly before gelation. The chest was closed and the rat was allowed to recover. After 4 weeks, all animals were sacrificed and hearts were harvested for histological and immunohistochemical evaluation.

2.6. Echocardiography

Echocardiography was performed 2 days before surgery (baseline) and at 2, 14, and 28 days post-MI surgery to evaluate cardiac function. Short-axis videos of the left ventricle (LV) by B-mode were obtained using a Vevo 770 high-resolution *in vivo* micro-Imaging system (Visual Sonics, Ontario, Canada). End-systolic area (ESA) and end-diastolic area (EDA) were measured using NIH ImageJ 1.46r and fractional area change (FAC) was calculated as $[(EDA-ESA)/EDA]*100\%$. Percent improvements of one group over another were calculated as the difference between the % drops in FAC values of the first and second groups divided by the higher % drop of the two groups.

2.7. Histological analysis

At 4 weeks post-infarction, rats were sacrificed by injecting 2 ml of deionized (DI) water saturated with potassium chloride (KCl) (Sigma Aldrich, St. Louis, MO) in the LV to arrest the heart in diastole. Hearts were harvested and frozen in OCT compound. Specimens were

sectioned at 6 mm thickness from apex to the ligation level with 500 μm intervals. Sections were fixed in 2–4% paraformaldehyde (fisher Scientific, Fair Lawn, NJ) prior to all staining procedures.

Hematoxylin and eosin (H&E) staining was performed for general evaluation. Five to six H&E stained slides from each group were randomly selected and the ventricular wall thickness in the infarct zone of each was measured near the mid-section level of the infarct tissue using NIS Elements AR imaging software (Nikon Instruments, Melville, NY).

For assessment of fibrosis, picosirius red staining was used to stain collagen fibers. The fraction area of collagen deposition in the infarct region was measured by NIS Elements AR software. Five to six slides from each group were used for quantification near the mid-section level of the infarct tissue.

2.8. Immunohistochemical analysis

For evaluation of inflammation, a mouse anti-rat CD68 (Millipore, Temecula CA) was used followed by an Alexa fluor 594 goat anti-mouse antibody (Invitrogen, Carlsbad, CA). For evaluation of angiogenesis, ECs were detected by a rabbit anti-rat Von Willebrand factor (vWF) antibody (US Abcam, Cambridge, MA) followed by an Alexa fluor 594 goat anti-rabbit antibody (Invitrogen Carlsbad, CA). Mural cells were detected by a FITC-conjugated anti- α - smooth muscle actin (α -SMA) monoclonal antibody (Sigma Aldrich, St. Louis, MO). Viable cardiomyocytes were detected by staining using a mouse anti-rat cardiac troponin I (cTnI) antibody (US Abcam, Cambridge, MA) followed by an Alexa fluor 488 goat anti-mouse antibody (Invitrogen, Carlsbad, CA). All slides were last counterstained with DAPI (Invitrogen, Carlsbad, CA).

For quantification, four to five slides from each group were utilized near the midsection level of the infarct tissue. The numbers of CD68-positive cells and vWF- and α -SMA-positive vessels were counted and reported per mm^2 areas. The cTnI-positive fraction area in the infarct region was measured by NIS Elements AR software. Intensity of fluorescence was determined by ImageJ and normalized to the background value.

2.9. Statistical analysis

Results are presented as means \pm standard deviations (SD). GraphPad Prism 5.0 statistical software (La Jolla, CA) was used for statistical analysis. One-way ANOVA followed by Tukey's SD test was used for *in vitro* assays, histological and immunohistochemical analyses. Two-way ANOVA followed by Bonferroni post-hoc test was used for echocardiography analysis. P value < 0.05 was considered significantly different.

3. Results

3.1. Fibrin gel-coacervate system achieves sequential delivery

Previously, we studied VEGF release from the coacervate which was relatively slow because of its mid-range affinity for heparin ($k_d=165$ nM) [25, 38]. With a weaker heparin-binding affinity ($k_d=752$ nM) [39], PDGF release from the coacervate occurs faster than for VEGF (supplemental Fig. S1). A proper therapeutic angiogenesis process needs a sequential

release of VEGF first followed by PDGF. In order to obtain faster VEGF release, we embedded it in a fibrin gel without loading it into the coacervate. We then loaded PDGF in the coacervate to provide its sustained release and embedded it in the same fibrin gel (Fig. 1A). The loading efficiencies were 87% for VEGF and 97% for PDGF as observed 1 hour after loading. VEGF had a burst release of 44% including the unloaded amount by day 1, while PDGF had a minimal burst release of 14% (Fig. 1B). Having a significant release of VEGF by day 1 might prove beneficial for angiogenesis and heart function after MI [40]. This delivery system achieved sequential release kinetics, where 95% of VEGF was released by one week and only 40% of PDGF, which continued to release up to 75% after three weeks (Fig. 1B). The *in vivo* release rate can be further influenced by fibrinolysis, hydrolytic degradation of the PEAD polycation, enzymatic degradation by esterases and heparinases, and dissociation of the coacervate in an ionic environment. Thus, *in vivo* release is expected to be faster. Overall, the release kinetics attained with the fibrin gel-coacervate delivery vehicle may enhance the formation of neovasculature based on the physiological roles of VEGF and PDGF during angiogenesis [15, 17].

3.1. PDGF coacervate induces SMC chemotaxis and proliferation

We reported previously on VEGF bioactivity in free form and using the coacervate [25]. Here, we evaluated the effect of PDGF released from the coacervate on SMC migration using a Boyden chamber assay. Free PDGF induced significantly more SMC migration compared to controls, however the same dose of PDGF delivered by the coacervate had the greatest chemotactic effect compared to all groups (Fig. 2A,B). The empty vehicle was also demonstrated to be inert with no effect on cell migration compared to basal media alone.

We also tested the effect of coacervate-released PDGF on SMC proliferation using a BrdU assay. Again, we observed no significant effect of the vehicle compared to basal media control. Both free PDGF and PDGF coacervate induced significant SMC proliferation compared to control groups. However, PDGF coacervate also increased cell proliferation compared to free PDGF (Fig. 2C). Collectively, these results demonstrate that PDGF released from the PEAD coacervate is highly bioactive and can stimulate proliferation and migration of SMCs *in vitro*.

3.2. Sequential delivery improves EC proliferation and vessel sprouting

In order to evaluate the potential benefit of sequential release of VEGF and PDGF, we performed EC proliferation and aortic ring vessel sprouting assays. We hypothesized that high initial PDGF concentrations would reduce the effect of VEGF on ECs. Free VEGF +PDGF induced significantly more proliferation than basal media, but not more than empty vehicle, which showed no difference compared to basal media. However, sequentially delivered VEGF+PDGF induced significantly more proliferation than both control and free GFs (Fig. 3A).

In the aortic ring assay, free GFs induced significantly more microvessel outgrowth and longer sprouts from ring segments compared to basal media but not compared to empty vehicle. In contrast, sequential delivery showed significantly larger sprouting area than all groups (Fig. 3B,C). Taken together, these experiments suggest that PDGF has an

antagonistic effect on VEGF-mediated angiogenic responses *in vitro* which can be avoided by a sequential delivery approach.

3.3. Sequential delivery of VEGF and PDGF improves overall cardiac function

We next evaluated the *in vivo* effect of sequential delivery in a rat MI model comparing saline, empty vehicle, free VEGF+PDGF, and sequentially delivered VEGF+PDGF. We evaluated changes in LV contractility using 2-D echocardiography and reported heart function as fractional area change (FAC). ESA and EDA values were similar for all groups suggesting little to no effect on ventricular dilation over the time period evaluated (Fig. 4A,B).

MI induction was confirmed by a significant drop in FAC 2 days after infarction (Fig. 4C). No significant differences were found between groups at baseline or at day 2. At 2 weeks, sequential delivery group showed a significant improvement in cardiac function compared to all other groups. FAC values were $32.5 \pm 3.3\%$ for saline, $34.9 \pm 5\%$ for empty vehicle, $36 \pm 2.6\%$ for free GFs, and $45.6 \pm 2.5\%$ for sequential delivery (Fig. 4C). No significant differences were found between saline, empty vehicle, and free GFs values at 2 weeks. This result represented a 60% improvement by sequential delivery over free GFs and 68% over saline.

At 4 weeks, FAC declined slightly for all groups, but sequential delivery group maintained its improvement in cardiac function with a significantly higher FAC compared to all groups. FAC values were $30 \pm 4.3\%$ for saline, $32.2 \pm 2.8\%$ for empty vehicle, $33.9 \pm 4.4\%$ for free GFs groups, and $44.4 \pm 3.2\%$ for sequential delivery (Fig. 4C). The sequential delivery value represented a 59% improvement over free GFs and 66% over saline. The ability of sequential delivery to improve and maintain the cardiac function 4 weeks after MI stresses the importance of spatiotemporal presentation towards the effectiveness of VEGF and PDGF.

3.4. Sequential delivery increases ventricular wall thickness and reduces fibrosis in the infarcted myocardium

After evaluation of overall cardiac function, we performed investigations at the tissue level using histology and immunohistochemistry. At 4 weeks, H&E stained tissue showed increased granulated scar tissue areas with thinner LV walls in the infarct region in saline ($591.2 \pm 55.1 \mu\text{m}$), empty vehicle ($630 \pm 135.1 \mu\text{m}$), and free GFs ($797.9 \pm 144.3 \mu\text{m}$) groups with no significant differences in wall thicknesses between them. In contrast, sequential delivery showed significantly increased LV wall thickness ($1205.7 \pm 224.9 \mu\text{m}$) compared to all groups with less scar tissue and granulation replacing normal cardiac muscle (Fig. 5A,B).

The extent of fibrosis was assessed using picosirius red staining. Collagen deposition was quantified and found to be significantly less in the sequential delivery group compared to all other groups which contained dense deposition of fibrillar collagen along the LV wall and extended to the infarct border zone (Fig. 5C,D). The area fractions of collagen deposition were $36.4 \pm 12.1\%$ for saline, $32 \pm 6.6\%$ for empty vehicle, $31.4 \pm 3.2\%$ for free GFs, and

19 ± 3.8% for sequential delivery (Fig. 5C). The reduced fibrosis and LV wall thinning due to sequential delivery of VEGF and PDGF is likely a contributing factor to the enhanced cardiac contractility since less fibrotic tissue reduces the stiffening of the ventricular walls and the extent of cardiac remodeling that occurs after MI [41].

3.5. Sequential delivery provides persistent angiogenesis in the infarcted myocardium

Restoring blood flow to the infarcted myocardium through robust angiogenesis is key to tissue regeneration and functional recovery. To investigate the development of mature and stable vasculature in the infarct region, we stained for the EC marker vWF and pericyte marker α -SMA (Fig. 6A). In addition to being an EC marker, vWF is a marker of cell homeostasis [42] and can be used to evaluate the functionality of new blood vessels. After 4 weeks, free GFs group (25.6 ± 3.2 per mm^2) showed a significantly higher number of vWF-positive vessels in comparison to saline (15.5 ± 3.1 per mm^2) and empty vehicle (15.7 ± 3 per mm^2) groups which showed only few vessels in the infarct zone (Fig. 6A,B). In contrast, sequential delivery (49.6 ± 8.1 per mm^2) showed an increase in vWF-positive vessels that was significantly higher than all groups. This suggests that sequential release of VEGF and PDGF helped improve the formation of neovessels with increased functionality.

The stability and maturity of new vasculature and prevention of its regression is very important for successful ischemic tissue repair. The goal of therapeutic angiogenesis is therefore to produce neovasculature that is not transient but rather is long-term, stable, mature, and robust. To examine the maturity of neovessels, we stained for α -SMA to detect pericytes associated with newly formed vWF-positive vessels (Fig. 6A). Few α -SMA-positive vessels were found in saline (6.9 ± 1.3 per mm^2), empty vehicle (6.5 ± 1.9 per mm^2), and free GFs (8.9 ± 2.7 per mm^2) groups with no statistical difference among them. On the other hand, sequential delivery showed many α -SMA-positive vessels (25.5 ± 8.7 per mm^2) likely due to the recruitment of pericytes by PDGF released in a sustained manner by the fibrin gel-coacervate delivery system (Fig. 6A,C). These results indicate the formation of stable and mature neovessels including capillaries and arterioles that are likely involved in tissue perfusion. This robust angiogenesis process is seemingly a key factor in the observed improvement of cardiac contractility at the functional level.

3.6. Sequential delivery maintains cardiac viability in the infarcted myocardium

Cardiomyocyte survival is essential to maintain proper contractile function of the LV after MI. The viability of the cardiac muscle in the infarcted myocardium was examined by staining for cardiomyocyte marker cTnI (Fig. 7A). At 4 weeks, Saline, empty vehicle, and free GFs groups showed reduced cardiomyocyte survival in the infarct region with cTnI-positive area fractions of $30.5 \pm 7.4\%$, $29.4 \pm 11\%$, and $27.4 \pm 3.7\%$, respectively (Fig. 7A,B). There was no statistical differences noted among the three groups. In contrast, sequential delivery showed a significantly higher cTnI-positive area fraction ($55.6 \pm 18.2\%$) than all groups suggesting better viability and preservation of the cardiac myofibers which help in the improvement of overall cardiac function (Fig. 7A,B).

3.7. Sequential delivery reduces inflammation in the infarcted myocardium

Reducing inflammation triggered by MI is an important goal towards recovery and repair of the myocardium [43]. Local inflammation in the infarct zone was evaluated by staining for a pan-macrophage marker, CD68. At 4 weeks, we observed that both free GFs and sequential delivery groups greatly reduced the presence of macrophages (Fig. 7C,D). Sequential delivery group showed many less CD68-positive cells (48.9 ± 12.4 per mm^2) than free GFs group (113.6 ± 28.2 per mm^2), however no statistical difference was found between the two, though a trend is clearly observed. Saline (196.2 ± 44.4 per mm^2) and empty vehicle (204.2 ± 52.7 per mm^2) groups showed significantly higher numbers of CD68-positive cells (Fig. 7C,D). This result suggests an indirect role for VEGF and/or PDGF in reducing macrophage infiltration into the infarct zone after MI possibly due to reduced tissue damage or down-regulation of pro-inflammatory cytokines.

4. Discussion

With the aim of promoting tissue repair and functional recovery, restoring the blood supply to ischemic tissues through therapeutic angiogenesis remains an exciting route. VEGF and PDGF are potent angiogenic factors with relatively distinct roles [17]. One key to successful therapeutic angiogenesis is careful consideration of the spatiotemporal profiles of administered GFs. It has been shown that VEGF can inhibit PDGF signaling where VEGFR-2, activated by VEGF, complexes with PDGFR- β to block its signal transduction, thus compromising its role in pericyte recruitment and neovessel stabilization [22]. One study using synthetic modified RNA encoding human VEGF concluded that VEGF administration can effectively improve heart function when present for just 2 days after MI [40]. This strongly suggests that certain GFs are only needed in the early stage of angiogenesis, while others should be present in the later stages.

Administration of various angiogenic GFs has been studied for a long time [3, 5, 6]. However, most strategies showed limited therapeutic effect because they focus on delivering single GFs involved in the early stages of angiogenesis, while overlooking the importance of stabilizing the sprouting neovessels through the actions of late-stage GFs [10, 12, 17]. With a more comprehensive understanding of the mechanisms of angiogenesis, researchers realized the need to administer more than one GF in their therapeutic strategies [10]. However, these therapies still demonstrated low efficacy when important factors such as the spatiotemporal presentation and protection of GFs were not considered. One study found that combinatorial plasmid gene transfer of VEGF and PDGF did not improve angiogenesis more than single plasmid treatments did in infarcted rat myocardium [44]. Another study concluded that bolus injections of a cocktail of four GFs: FGF-2, stromal-derived factor 1- α (SDF1- α), insulin growth factor-1 (IGF-1), and hepatocyte growth factor (HGF), did not improve cardiac function, reduce infarct size, or promote stable microvasculature [45]. When the shortcomings of bolus injections were realized, investigators shifted their focus towards controlled delivery vehicles capable of sequential and spatiotemporal presentation of GFs. Factors such as GF loading efficiency, spatiotemporal profiles, burst releases, control over release kinetics, GF bioactivity and bioavailability, and cost of manufacturing are challenges that should be addressed to create an effective delivery system [10, 12, 26,

46, 47]. Several systems demonstrated the ability to sequentially deliver two GFs, however they are not injectable, and thus difficult to apply towards treating heart diseases [21, 48–50]. Others were able to develop injectable platforms that displayed the benefit of sequential delivery using various GFs and *in vivo* models [51–54].

In studies where an early-stage factor was presented first followed by a late-stage factor, improved angiogenic responses over single factors or non-sequential delivery were observed. For example, when presented simultaneously, PDGF-BB and Ang1 inhibited the VEGF and Ang2-mediated EC sprouting and pericyte detachment *in vitro* and microvessel formation in a subcutaneous implant *in vivo* model; yet presentation of PDGF-BB and Ang1 at a later stage enhanced the angiogenic process [21]. Similarly, when applied together, FGF-2 and PDGF-BB were shown to inhibit each other; however, sequential delivery of FGF-2 followed by PDGF-BB improved EC migration, EC and vascular pericyte colocalization, and functional angiogenesis in a subcutaneous implant model [23]. These results are in support of our *in vitro* findings regarding antagonism between VEGF and PDGF signaling. Therefore, in order to achieve a robust angiogenic response, therapies must take into consideration the multiple GFs involved, their spatiotemporal cues in the natural tissue microenvironment, and the translational potential of the delivery platform.

The delivery system described in this study is based on a combination of fibrin gel and a complex coacervate for sequential delivery of VEGF followed by PDGF. The coacervate contains heparin and a biocompatible polycation, PEAD, which closely and advantageously imitates the native signaling environment involving extracellular matrix proteoglycans, ligands, and cell receptors [33, 55–57]. This vehicle can protect the GFs from rapid enzymatic degradation and potentiate their bioactivities [24, 25, 27–33]. In this study, we demonstrated that the fibrin gel-coacervate system achieved early release of VEGF to trigger EC proliferation and sprouting and delayed release of PDGF to recruit pericytes that stabilize the newly formed vessels. Even though PDGF is still present in the early stage, our delivery system largely limited its overlap with VEGF presence and thus limited the antagonism between the two factors. Our *in vitro* assays demonstrated that PDGF coacervate significantly improved SMC proliferation and migration compared to free PDGF. We also showed the importance of sequential delivery of VEGF followed by PDGF towards EC proliferation by limiting PDGF-mediated inhibition of VEGF angiogenic effects, in accordance with previous reports [21–23]. The benefit of sequential release was further demonstrated by improved microvasculature sprouting from rat aortic rings.

In vivo, we demonstrated using a rat MI model that the fibrin gel-coacervate system led to a robust angiogenic response with extensive formation of mature and functional blood vessels in the infarct zone. We observed a significant increase in the number of vWF- and α -SMA positive vessels reflecting the formation of new stable and mature vasculature. Our results further demonstrate a reduction in myocardial fibrosis which mitigates the loss in contractile function seen in control groups [41, 43]. Moreover, cardiomyocyte survival, essential for preserving contractile function, was improved as a result of sequential delivery of VEGF and PDGF. Several variables not investigated in this study may have played a role in the improvement of cardiomyocyte survival and angiogenesis. For example, VEGF has been shown to elevate the levels of nitric oxide [58, 59], which is a potent vasodilator and an

endothelial survival factor that prevents apoptosis and improves EC proliferation and migration [60]. Vasodilation soon after infarction may improve cardiomyocyte survival. VEGF also improves FGF-2-mediated angiogenesis [20] and induces the release of SDF1- α which promotes cardiac stem cell and other progenitor cell mobilization to the infarct region [61]. In addition to its role in stabilizing neovessels, PDGF can also activate cardioprotective signaling pathways in cardiomyocytes [18]. Maintaining a viable cardiac muscle is essential to improving cardiac function after MI as demonstrated in studies attempting to stimulate proliferation of cardiomyocytes, prevent their apoptosis, and recruit cardiac progenitor cells to the heart [62–68]. Moreover, we demonstrated that sequential delivery of VEGF and PDGF reduced the presence of macrophages in the infarct zone 4 weeks after MI. This reduction might be due to indirect VEGF and/or PDGF down-regulation of proinflammatory cytokines. It is also possible that the improved angiogenesis and better preservation of cardiac muscle observed in our study reduced tissue damage, which may have in turn reduced inflammation. The culmination of these many benefits was reflected on a functional level by improved cardiac contractility as early as 2 weeks after infarction with approximately 60% improvement over free GF delivery.

Many studies have investigated different types of delivery vehicles for spatiotemporal control over the release or expression of two or more GFs [21, 23, 48–50, 53, 54, 69–72]; however very few have been tested in an animal model of MI [51, 52, 73]. In the one study testing sequential delivery of VEGF and PDGF in the infarcted myocardium, an increased systolic velocity-time integral, a measure of displacement of the myocardium during contraction, was reported but surprisingly no significant improvement in ejection fraction or LV end-systolic dimension was observed compared to saline control or single GF delivery [51]. Our study demonstrates significantly improved cardiac function through the measurement of LV contractility based on the FAC parameter, which is similar to ejection fraction but is a two-dimensional measurement. This functional improvement is corroborated by comprehensive histological and immunohistochemical analyses showing the beneficial effects of sequential delivery of VEGF and PDGF at the tissue level of the infarct region.

5. Conclusions

This study demonstrated that sequential controlled release of VEGF₁₆₅ and PDGF-BB can trigger the formation and stabilization of neovasculature, and improve cardiac function after MI in a rat model. The improvement is observed at 2 weeks and maintained at a similar level at 4 weeks. Improvements at the tissue level include increased mature blood vessel formation, cardiomyocyte survival, and decreased collagen deposition and inflammation in the infarct zone. These results suggest that the fibrin gel-coacervate delivery system can induce robust angiogenesis, reduce scar burden, and potentially halt the pathological progression post MI. This controlled delivery approach warrants further investigation in a clinically-relevant large animal model.

Supplementary Material

Refer to Web version on PubMed Central for supplementary material.

Acknowledgements

The authors would like to thank Scientific Protein Labs for donating clinical-grade heparin. This research is supported by the biomechanics in regenerative medicine (BiRM) T32 training program (grant # 5T32EB003392-09) of the National Institutes of Health, the American Heart Association (grant # 12EIA9020016), and the National Science Foundation (grant # DMR-1005766).

References

1. Go AS, Mozaffarian D, Roger VL, Benjamin EJ, Berry JD, Blaha MJ, Dai S, Ford ES, Fox CS, Franco S, Fullerton HJ, Gillespie C, Hailpern SM, Heit JA, Howard VJ, Huffman MD, Judd SE, Kissela BM, Kittner SJ, Lackland DT, Lichtman JH, Lisabeth LD, Mackey RH, Magid DJ, Marcus GM, Marelli A, Matchar DB, McGuire DK, Mohler ER 3rd, Moy CS, Mussolino ME, Neumar RW, Nichol G, Pandey DK, Paynter NP, Reeves MJ, Sorlie PD, Stein J, Towfighi A, Turan TN, Virani SS, Wong ND, Woo D, Turner MB. C. American Heart Association Statistics, S. Stroke Statistics, Heart disease and stroke statistics--2014 update: a report from the American Heart Association. *Circulation*. 2014; 129:e28–e292. [PubMed: 24352519]
2. Kurrelmeier K, Kalra D, Bozkurt B, Wang F, Dibbs Z, Seta Y, Baumgarten G, Engle D, Sivasubramanian N, Mann DL. Cardiac remodeling as a consequence and cause of progressive heart failure. *Clinical Cardiology*. 1998; 21:14–19.
3. Cochain C, Channon KM, Silvestre JS. Angiogenesis in the infarcted myocardium. *Antioxid Redox Signal*. 2013; 18:1100–1113. [PubMed: 22870932]
4. Devezza L, Choi J, Yang F. Therapeutic angiogenesis for treating cardiovascular diseases. *Theranostics*. 2012; 2:801–814. [PubMed: 22916079]
5. Segers VF, Lee RT. Protein therapeutics for cardiac regeneration after myocardial infarction. *J Cardiovasc Transl Res*. 2010; 3:469–477. [PubMed: 20607468]
6. Formiga FR, Tamayo E, Simon-Yarza T, Pelacho B, Prosper F, Blanco-Prieto MJ. Angiogenic therapy for cardiac repair based on protein delivery systems. *Heart Fail Rev*. 2012; 17:449–473. [PubMed: 21979836]
7. Hwang H, Kloner RA. Improving regenerating potential of the heart after myocardial infarction: factor-based approach. *Life Sci*. 2010; 86:461–472. [PubMed: 20093126]
8. Zachary I, Morgan RD. Therapeutic angiogenesis for cardiovascular disease: biological context, challenges, prospects. *Heart*. 2011; 97:181–189. [PubMed: 20884790]
9. Li WW, Talcott KE, Zhai AW, Kruger EA, Li VW. The role of therapeutic angiogenesis in tissue repair and regeneration. *Adv Skin Wound Care*. 2005; 18:491–500. quiz 501-492. [PubMed: 16365547]
10. Chen FM, Zhang M, Wu ZF. Toward delivery of multiple growth factors in tissue engineering. *Biomaterials*. 2010; 31:6279–6308. [PubMed: 20493521]
11. Chu H, Wang Y. Therapeutic angiogenesis: controlled delivery of angiogenic factors. *Ther Deliv*. 2012; 3:693–714. [PubMed: 22838066]
12. Tayalia P, Mooney DJ. Controlled growth factor delivery for tissue engineering. *Adv Mater*. 2009; 21:3269–3285. [PubMed: 20882497]
13. Epstein SE, Kornowski R, Fuchs S, Dvorak HF. Angiogenesis therapy: amidst the hype, the neglected potential for serious side effects. *Circulation*. 2001; 104:115–119. [PubMed: 11435348]
14. Lee RJ, Springer ML, Blanco-Bose WE, Shaw R, Ursell PC, Blau HM. VEGF gene delivery to myocardium: deleterious effects of unregulated expression. *Circulation*. 2000; 102:898–901. [PubMed: 10952959]
15. Betsholtz C. Insight into the physiological functions of PDGF through genetic studies in mice. *Cytokine Growth Factor Rev*. 2004; 15:215–228. [PubMed: 15207813]
16. Eklund L, Olsen BR. Tie receptors and their angiopoietin ligands are context-dependent regulators of vascular remodeling. *Exp Cell Res*. 2006; 312:630–641. [PubMed: 16225862]
17. Carmeliet P, Jain RK. Molecular mechanisms and clinical applications of angiogenesis. *Nature*. 2011; 473:298–307. [PubMed: 21593862]

18. Hsieh PC, Davis ME, Gannon J, MacGillivray C, Lee RT. Controlled delivery of PDGF-BB for myocardial protection using injectable self-assembling peptide nanofibers. *J Clin Invest.* 2006; 116:237–248. [PubMed: 16357943]
19. Ferrara N, Gerber HP, LeCouter J. The biology of VEGF and its receptors. *Nat Med.* 2003; 9:669–676. [PubMed: 12778165]
20. Maulik N, Thirunavukkarasu M. Growth factors and cell therapy in myocardial regeneration. *J Mol Cell Cardiol.* 2008; 44:219–227. [PubMed: 18206905]
21. Brudno Y, Ennett-Shepard AB, Chen RR, Aizenberg M, Mooney DJ. Enhancing microvascular formation and vessel maturation through temporal control over multiple pro-angiogenic and pro-maturation factors. *Biomaterials.* 2013; 34:9201–9209. [PubMed: 23972477]
22. Greenberg JI, Shields DJ, Barillas SG, Acevedo LM, Murphy E, Huang J, Schepcke L, Stockmann C, Johnson RS, Angle N, Cheresh DA. A role for VEGF as a negative regulator of pericyte function and vessel maturation. *Nature.* 2008; 456:809–813. [PubMed: 18997771]
23. Tengood JE, Ridenour R, Brodsky R, Russell AJ, Little SR. Sequential delivery of basic fibroblast growth factor and platelet-derived growth factor for angiogenesis. *Tissue Eng Part A.* 2011; 17:1181–1189. [PubMed: 21142700]
24. Chu H, Johnson NR, Mason NS, Wang Y. A [polycation:heparin] complex releases growth factors with enhanced bioactivity. *J Control Release.* 2011; 150:157–163. [PubMed: 21118705]
25. Awada HK, Johnson NR, Wang Y. Dual delivery of vascular endothelial growth factor and hepatocyte growth factor coacervate displays strong angiogenic effects. *Macromol Biosci.* 2014; 14:679–686. [PubMed: 24452960]
26. Vasita R, Katti DS. Growth factor-delivery systems for tissue engineering: a materials perspective. *Expert Rev Med Devices.* 2006; 3:29–47. [PubMed: 16359251]
27. Chu H, Gao J, Wang Y. Design, synthesis, and biocompatibility of an arginine-based polyester. *Biotechnol Prog.* 2012; 28:257–264. [PubMed: 22034156]
28. Chu H, Chen CW, Huard J, Wang Y. The effect of a heparin-based coacervate of fibroblast growth factor-2 on scarring in the infarcted myocardium. *Biomaterials.* 2013; 34:1747–1756. [PubMed: 23211448]
29. Chu H, Gao J, Chen CW, Huard J, Wang Y. Injectable fibroblast growth factor-2 coacervate for persistent angiogenesis. *Proc Natl Acad Sci U S A.* 2011; 108:13444–13449. [PubMed: 21808045]
30. Johnson NR, Wang Y. Controlled delivery of heparin-binding EGF-like growth factor yields fast and comprehensive wound healing. *J Control Release.* 2013; 166:124–129. [PubMed: 23154193]
31. Johnson NR, Wang Y. Controlled delivery of sonic hedgehog morphogen and its potential for cardiac repair. *PLoS One.* 2013; 8:e63075. [PubMed: 23690982]
32. Lee KW, Johnson NR, Gao J, Wang Y. Human progenitor cell recruitment via SDF-1alpha coacervate-laden PGS vascular grafts. *Biomaterials.* 2013; 34:9877–9885. [PubMed: 24060423]
33. Johnson NR, Wang Y. Coacervate delivery systems for proteins and small molecule drugs. *Expert Opin Drug Deliv.* 2014; 11:1829–1832. [PubMed: 25138695]
34. Black KA, Priftis D, Perry SL, Yip J, Byun WY, Tirrell M. Protein Encapsulation via Polypeptide Complex Coacervation. *ACS Macro Letters.* 2014; 3:1088–1091.
35. Aplin AC, Fogel E, Zorzi P, Nicosia RF. The aortic ring model of angiogenesis. *Methods Enzymol.* 2008; 443:119–136. [PubMed: 18772014]
36. Go RS, Owen WG. The rat aortic ring assay for in vitro study of angiogenesis. *Methods Mol Med.* 2003; 85:59–64. [PubMed: 12710197]
37. Dobner S, Bezuidenhout D, Govender P, Zilla P, Davies N. A synthetic non-degradable polyethylene glycol hydrogel retards adverse post-infarct left ventricular remodeling. *J Card Fail.* 2009; 15:629–636. [PubMed: 19700140]
38. Ashikari-Hada S, Habuchi H, Kariya Y, Itoh N, Reddi AH, Kimata K. Characterization of growth factor-binding structures in heparin/heparan sulfate using an octasaccharide library. *J Biol Chem.* 2004; 279:12346–12354. [PubMed: 14707131]
39. Freeman I, Kedem A, Cohen S. The effect of sulfation of alginate hydrogels on the specific binding and controlled release of heparin-binding proteins. *Biomaterials.* 2008; 29:3260–3268. [PubMed: 18462788]

40. Zangi L, Lui KO, von Gise A, Ma Q, Ebina W, Ptaszek LM, Spater D, Xu H, Tabebordbar M, Gorbato R, Sena B, Nahrendorf M, Briscoe DM, Li RA, Wagers AJ, Rossi DJ, Pu WT, Chien KR. Modified mRNA directs the fate of heart progenitor cells and induces vascular regeneration after myocardial infarction. *Nat Biotechnol.* 2013; 31:898–907. [PubMed: 24013197]
41. Sutton MG, Sharpe N. Left ventricular remodeling after myocardial infarction: pathophysiology and therapy. *Circulation.* 2000; 101:2981–2988. [PubMed: 10869273]
42. Tsai HM. von Willebrand factor, shear stress, and ADAMTS13 in hemostasis and thrombosis. *ASAIO J.* 2012; 58:163–169. [PubMed: 22370688]
43. Krishnamurthy P, Rajasingh J, Lambers E, Qin G, Losordo DW, Kishore R. IL-10 inhibits inflammation and attenuates left ventricular remodeling after myocardial infarction via activation of STAT3 and suppression of HuR. *Circ Res.* 2009; 104:e9–e18. [PubMed: 19096025]
44. Hao X, Mansson-Broberg A, Blomberg P, Dellgren G, Siddiqui AJ, Grinnemo KH, Wardell E, Sylven C. Angiogenic and cardiac functional effects of dual gene transfer of VEGF-A165 and PDGF-BB after myocardial infarction. *Biochem Biophys Res Commun.* 2004; 322:292–296. [PubMed: 15313205]
45. Hwang H, Kloner RA. The combined administration of multiple soluble factors in the repair of chronically infarcted rat myocardium. *J Cardiovasc Pharmacol.* 2011; 57:282–286. [PubMed: 21383589]
46. Lee K, Silva EA, Mooney DJ. Growth factor delivery-based tissue engineering: general approaches and a review of recent developments. *J R Soc Interface.* 2011; 8:153–170. [PubMed: 20719768]
47. Silva AK, Richard C, Bessodes M, Scherman D, Merten OW. Growth factor delivery approaches in hydrogels. *Biomacromolecules.* 2009; 10:9–18. [PubMed: 19032110]
48. Chen RR, Silva EA, Yuen WW, Mooney DJ. Spatio-temporal VEGF and PDGF delivery patterns blood vessel formation and maturation. *Pharm Res.* 2001; 24:258–264. [PubMed: 17191092]
49. Richardson TP, Peters MC, Ennett AB, Mooney DJ. Polymeric system for dual growth factor delivery. *Nat Biotechnol.* 2001; 19:1029–1034. [PubMed: 11689847]
50. Davies NH, Schmidt C, Bezuidenhout D, Zilla P. Sustaining neovascularization of a scaffold through staged release of vascular endothelial growth factor-A and platelet-derived growth factor-BB. *Tissue Eng Part A.* 2012; 18:26–34. [PubMed: 21895488]
51. Hao X, Silva EA, Mansson-Broberg A, Grinnemo KH, Siddiqui AJ, Dellgren G, Wardell E, Brodin LA, Mooney DJ, Sylven C. Angiogenic effects of sequential release of VEGF-A165 and PDGF-BB with alginate hydrogels after myocardial infarction. *Cardiovasc Res.* 2007; 75:178–185. [PubMed: 17481597]
52. Ruvinov E, Leor J, Cohen S. The promotion of myocardial repair by the sequential delivery of IGF-1 and HGF from an injectable alginate biomaterial in a model of acute myocardial infarction. *Biomaterials.* 2011; 32:565–578. [PubMed: 20889201]
53. Shin SH, Lee J, Lim KS, Rhim T, Lee SK, Kim YH, Lee KY. Sequential delivery of TAT-HSP27 and VEGF using microsphere/hydrogel hybrid systems for therapeutic angiogenesis. *J Control Release.* 2013; 166:38–45. [PubMed: 23262200]
54. Sun Q, Silva EA, Wang A, Fritton JC, Mooney DJ, Schaffler MB, Grossman PM, Rajagopalan S. Sustained release of multiple growth factors from injectable polymeric system as a novel therapeutic approach towards angiogenesis. *Pharm Res.* 2010; 27:264–271. [PubMed: 19953308]
55. Capila I, Linhardt RJ. Heparin-protein interactions. *Angew Chem Int Ed Engl.* 2002; 41:391–412. [PubMed: 12491369]
56. Mulloy B, Forster MJ. Conformation and dynamics of heparin and heparan sulfate. *Glycobiology.* 2000; 10:1147–1156. [PubMed: 11087707]
57. Pellegrini L. Role of heparan sulfate in fibroblast growth factor signalling: a structural view. *Curr Opin Struct Biol.* 2001; 11:629–634. [PubMed: 11785766]
58. Morbidelli L, Chang CH, Douglas JG, Granger HJ, Ledda F, Ziche M. Nitric oxide mediates mitogenic effect of VEGF on coronary venular endothelium. *Am J Physiol.* 1996; 270:H411–H415. [PubMed: 8769777]
59. van der Zee R, Murohara T, Luo Z, Zollmann F, Passeri J, Lekutat C, Isner JM. Vascular endothelial growth factor/vascular permeability factor augments nitric oxide release from

- quiescent rabbit and human vascular endothelium. *Circulation*. 1997; 95:1030–1037. [PubMed: 9054767]
60. Cooke JP, Losordo DW. Nitric oxide and angiogenesis. *Circulation*. 2002; 105:2133–2135. [PubMed: 11994243]
61. Tang JM, Wang JN, Zhang L, Zheng F, Yang JY, Kong X, Guo LY, Chen L, Huang YZ, Wan Y, Chen SY. VEGF/SDF-1 promotes cardiac stem cell mobilization and myocardial repair in the infarcted heart. *Cardiovasc Res*. 2011; 91:402–411. [PubMed: 21345805]
62. Bergmann O, Bhardwaj RD, Bernard S, Zdunek S, Barnabe-Heider F, Walsh S, Zupicich J, Alkass K, Buchholz BA, Druid H, Jovinge S, Frisen J. Evidence for cardiomyocyte renewal in humans. *Science*. 2009; 324:98–102. [PubMed: 19342590]
63. Bersell K, Arab S, Haring B, Kuhn B. Neuregulin1/ErbB4 signaling induces cardiomyocyte proliferation and repair of heart injury. *Cell*. 2009; 138:257–270. [PubMed: 19632177]
64. Braun T, Dimmeler S. Breaking the silence: stimulating proliferation of adult cardiomyocytes. *Dev Cell*. 2009; 17:151–153. [PubMed: 19686672]
65. Kuhn B, del Monte F, Hajjar RJ, Chang YS, Lebeche D, Arab S, Keating MT. Periostin induces proliferation of differentiated cardiomyocytes and promotes cardiac repair. *Nat Med*. 2007; 13:962–969. [PubMed: 17632525]
66. Abbott JD, Huang Y, Liu D, Hickey R, Krause DS, Giordano FJ. Stromal cell-derived factor-1alpha plays a critical role in stem cell recruitment to the heart after myocardial infarction but is not sufficient to induce homing in the absence of injury. *Circulation*. 2004; 110:3300–3305. [PubMed: 15533866]
67. Dhingra S, Sharma AK, Arora RC, Slezak J, Singal PK. IL-10 attenuates TNF-alpha-induced NF kappaB pathway activation and cardiomyocyte apoptosis. *Cardiovasc Res*. 2009; 82:59–66. [PubMed: 19181934]
68. Takehara N, Tsutsumi Y, Tateishi K, Ogata T, Tanaka H, Ueyama T, Takahashi T, Takamatsu T, Fukushima M, Komeda M, Yamagishi M, Yaku H, Tabata Y, Matsubara H, Oh H. Controlled delivery of basic fibroblast growth factor promotes human cardiosphere-derived cell engraftment to enhance cardiac repair for chronic myocardial infarction. *J Am Coll Cardiol*. 2008; 52:1858–1865. [PubMed: 19038683]
69. Choi DH, Subbiah R, Kim IH, Han DK, Park K. Dual growth factor delivery using biocompatible core-shell microcapsules for angiogenesis. *Small*. 2013; 9:3468–3476. [PubMed: 23585380]
70. Drinnan CT, Zhang G, Alexander MA, Pulido AS, Suggs LJ. Multimodal release of transforming growth factor-beta1 and the BB isoform of platelet derived growth factor from PEGylated fibrin gels. *J Control Release*. 2010; 147:180–186. [PubMed: 20381553]
71. Jiang B, Akar B, Waller TM, Larson JC, Appel AA, Brey EM. Design of a composite biomaterial system for tissue engineering applications. *Acta Biomater*. 2014; 10:1177–1186. [PubMed: 24321351]
72. Tengood JE, Kovach KM, Vescovi PE, Russell AJ, Little SR. Sequential delivery of vascular endothelial growth factor and sphingosine 1-phosphate for angiogenesis. *Biomaterials*. 2010; 31:7805–7812. [PubMed: 20674008]
73. Zhang H, Yuan YL, Wang Z, Jiang B, Zhang CS, Wang Q, Xu XH, Dong HY, Zhang ZM. Sequential, timely, and controlled expression of hVEGF165 and Ang-1 effectively improves functional angiogenesis and cardiac function in vivo. *Gene Ther*. 2013; 20:893–900. [PubMed: 23514706]

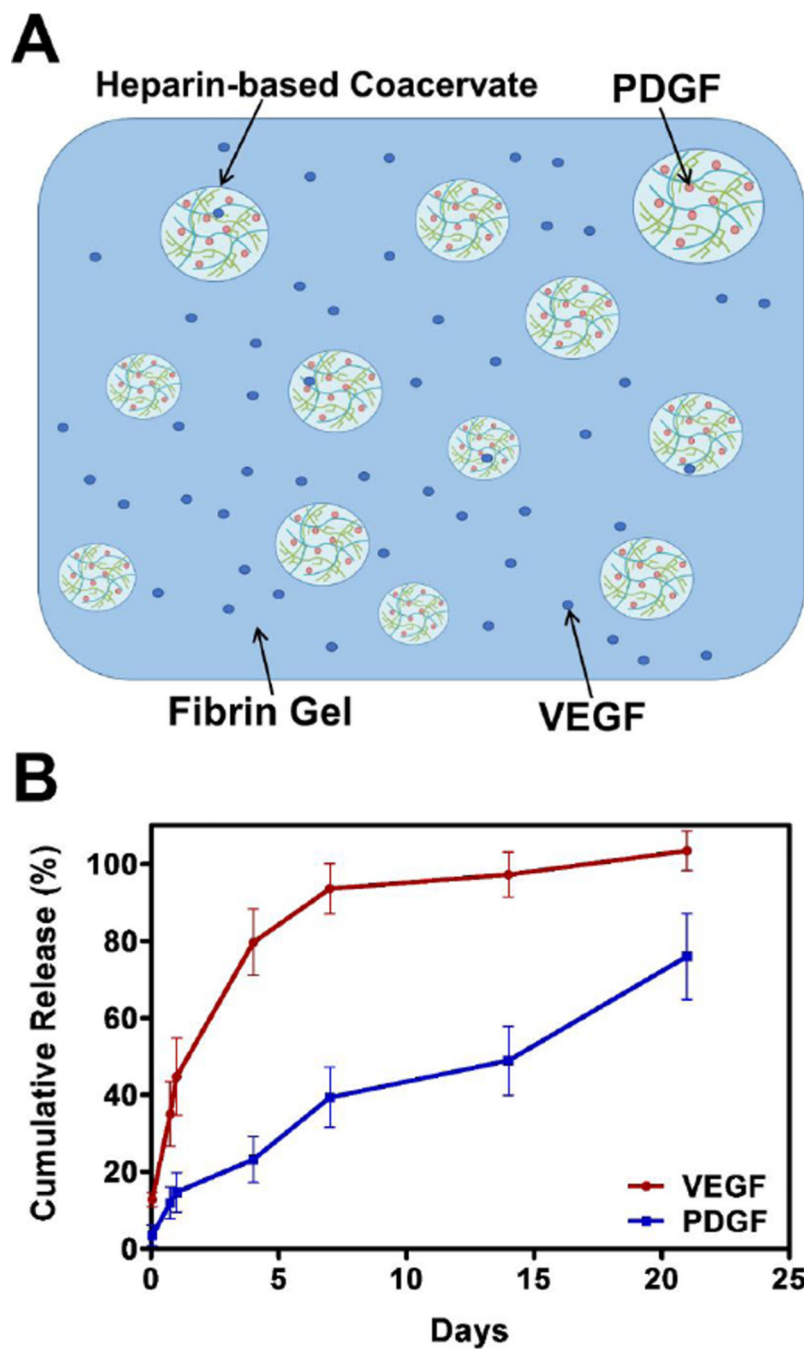


Fig. 1. Sequential delivery of VEGF and PDGF using a fibrin gel-coacervate system. (A) The delivery system was comprised of a fibrin gel embedding free VEGF and PDGF-loaded coacervate droplets. The coacervate was formed through electrostatic interactions by combining PDGF with heparin then with PEAD polycation (B) The delivery system described achieved sequential quick release of VEGF followed by a sustained release of PDGF. Data are presented as means \pm SD (n=3 per group).

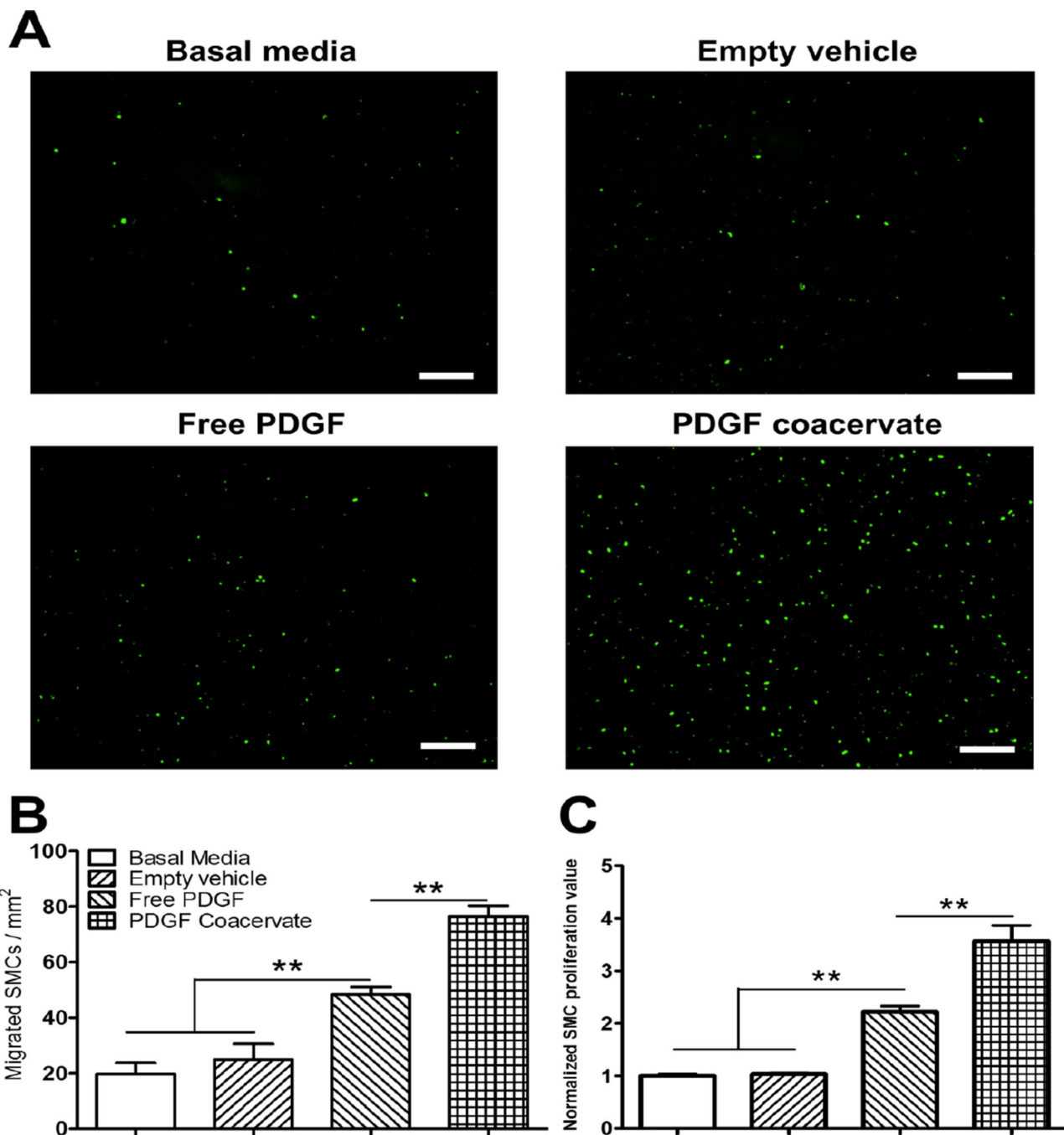


Fig. 2. PDGF cocervate promotes SMC chemotaxis and proliferation. (A) After 12h, images show more migrated SMC through the cell culture insert membrane towards PDGF cocervate compared to other groups. (B) Although free PDGF significantly induced migration compared to control, it was less than PDGF cocervate which significantly enhanced migration compared to all other groups. (C) After 48h, free PDGF induced significantly more SMC proliferation than controls, while PDGF cocervate induced significantly more

proliferation than all groups. Proliferation values were normalized to basal media average. Data are presented as means \pm SD (n=3 per group). ** $P < 0.01$. Scale bar=250 μ m.

Author Manuscript

Author Manuscript

Author Manuscript

Author Manuscript

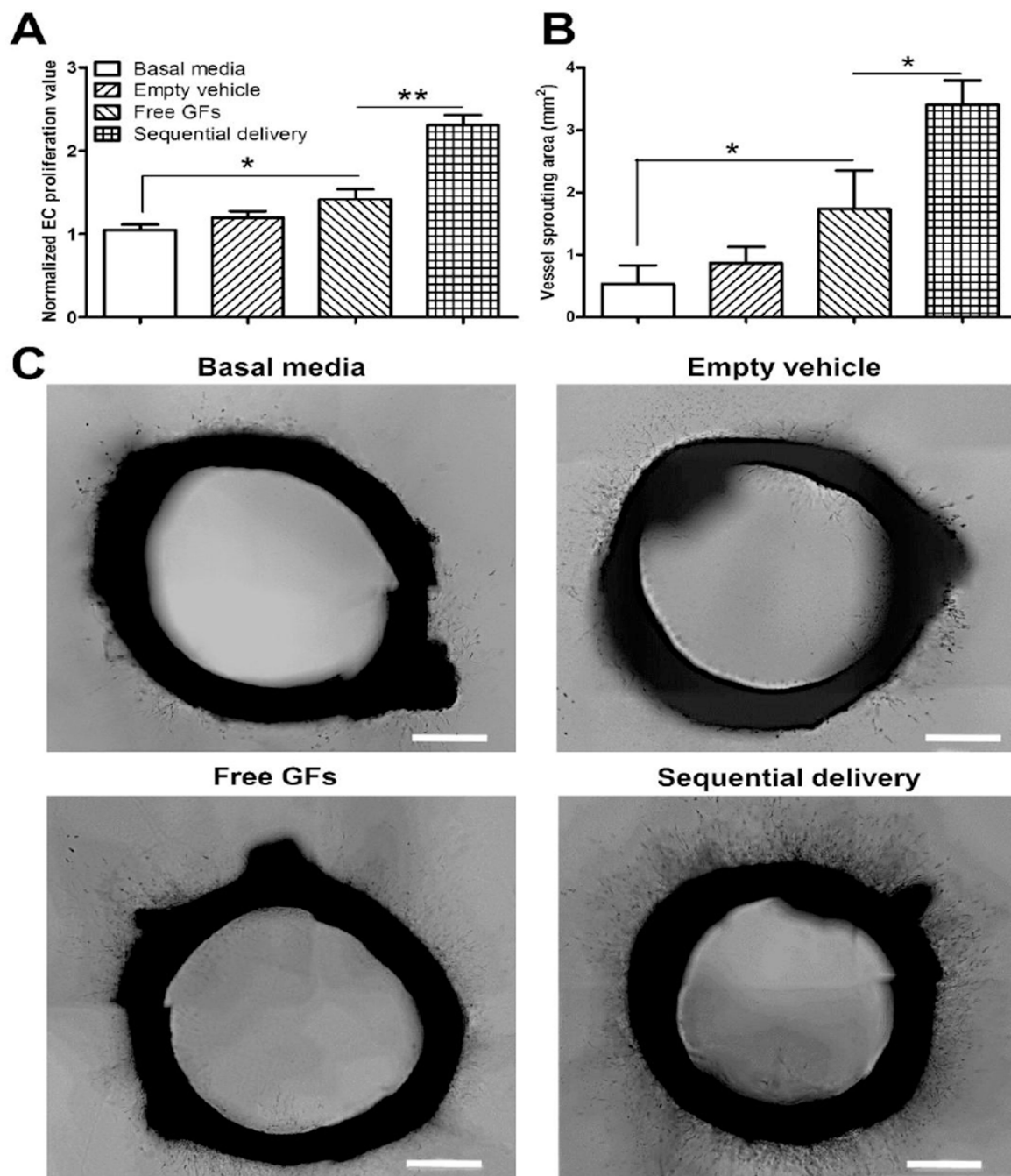


Fig. 3. Sequential delivery of VEGF and PDGF promotes endothelial cell proliferation and vessel sprouting. (A) After 48h, free GFs (VEGF+PDGF) induced significantly more endothelial proliferation than basal media, while sequential delivery of VEGF and PDGF induced significantly more proliferation than all groups. Proliferation values were normalized to basal media average. (B) After 6 days, rat aortic ring assay shows that free GFs induced significantly larger microvasculature sprouting area than basal media. Sequential delivery induced significantly larger sprouting areas compared to all groups. (C) Representative

images show microvasculature formation around rat aortic rings, with more sprouting observed in the sequential delivery group. Data are presented as means \pm SD (n=3 per group). * P <0.05, ** P <0.01. Scale bar=500 μ m.

Author Manuscript

Author Manuscript

Author Manuscript

Author Manuscript

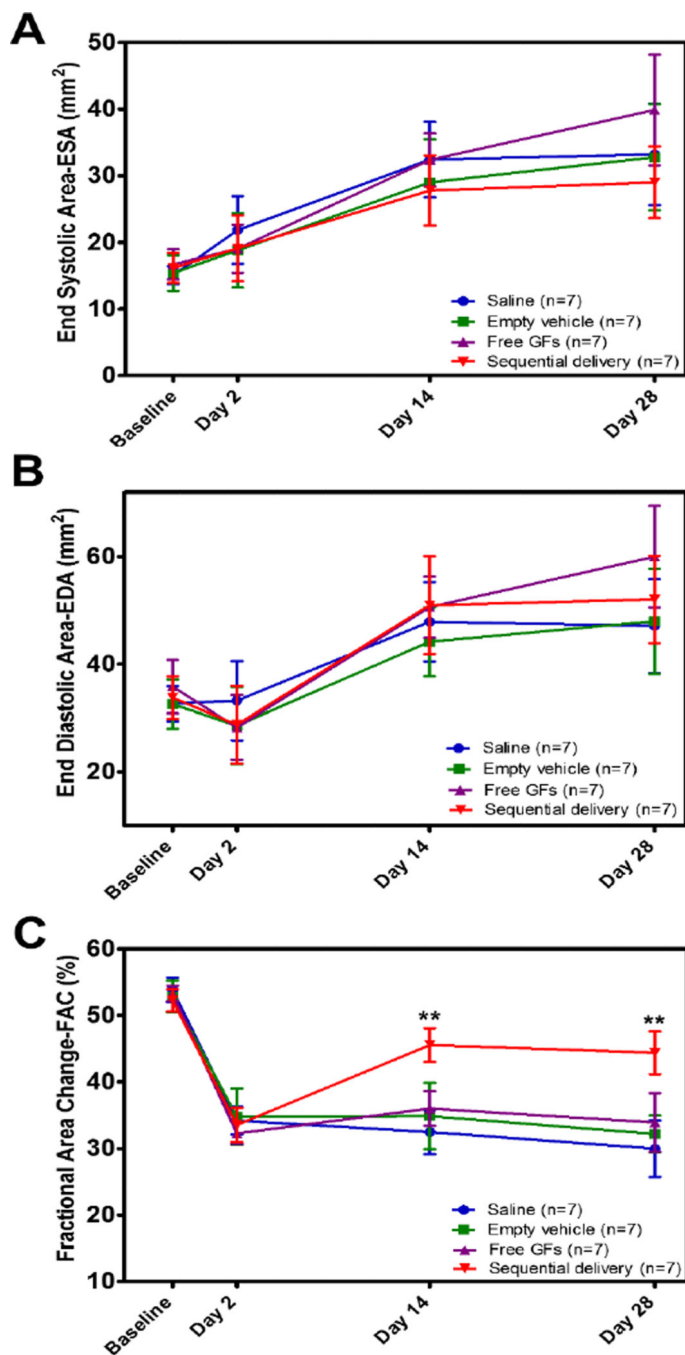


Fig. 4. Sequential delivery of VEGF and PDGF improves cardiac function after MI. (A) End-systolic area (ESA) and (B) End-diastolic area (EDA) showed no statistical difference between groups at all time points suggesting no effect on ventricular dilation. (C) % Fractional area change (FAC) reflected a significantly improved cardiac contractility at 2 wks and maintained at 4 wks in the sequential delivery group compared to all groups. In comparison, sequential delivery group displayed a 68% improvement over saline and 60% over free GFs at 2 wks. Data are presented as means \pm SD (n=7 per group). ** P <0.01.

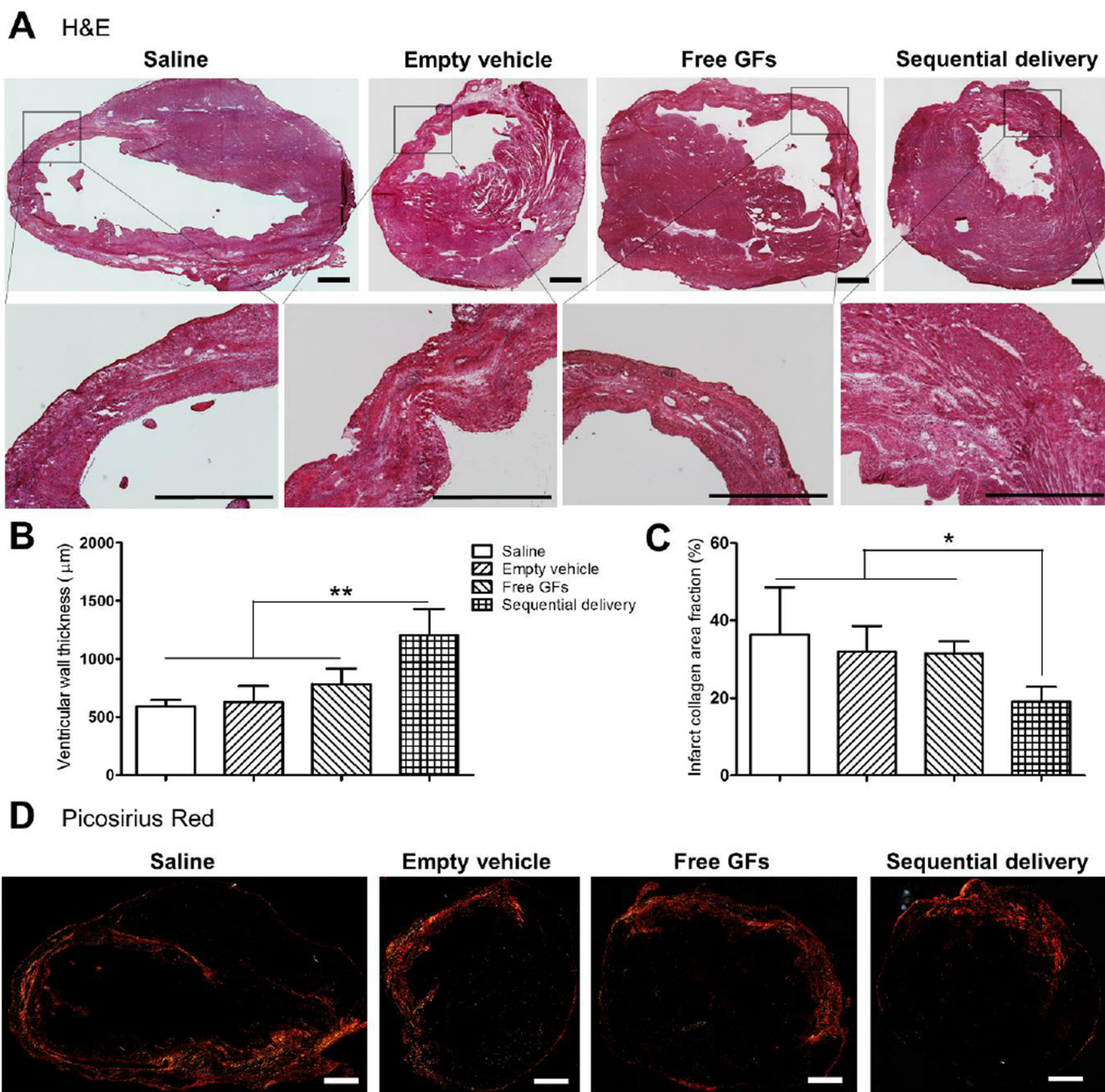


Fig. 5. Sequential delivery of VEGF and PDGF improves ventricular wall thickness and reduces fibrosis 4 wks after MI. (A) H&E staining showed ventricular wall thinning with damaged cardiac muscle surrounded by scar tissue in saline, empty vehicle, and free GFs groups. However, these damages were apparently alleviated in the sequential delivery group. Quantitative analysis showed (B) significantly increased ventricular wall thickness and (C) significantly reduced collagen deposition in the sequential delivery group compared to all groups. (D) Picosirius red staining images show the vast collagen deposition areas along the LV wall and infarct zone in saline, empty vehicle, and free GFs groups. Collagen deposition

was reduced in the sequential delivery group indicating less fibrotic tissue and scar formation. Data are presented as means \pm SD (n=5–6 per group). * P <0.05, ** P <0.01. Scale bar=1000 μ m.

Author Manuscript

Author Manuscript

Author Manuscript

Author Manuscript

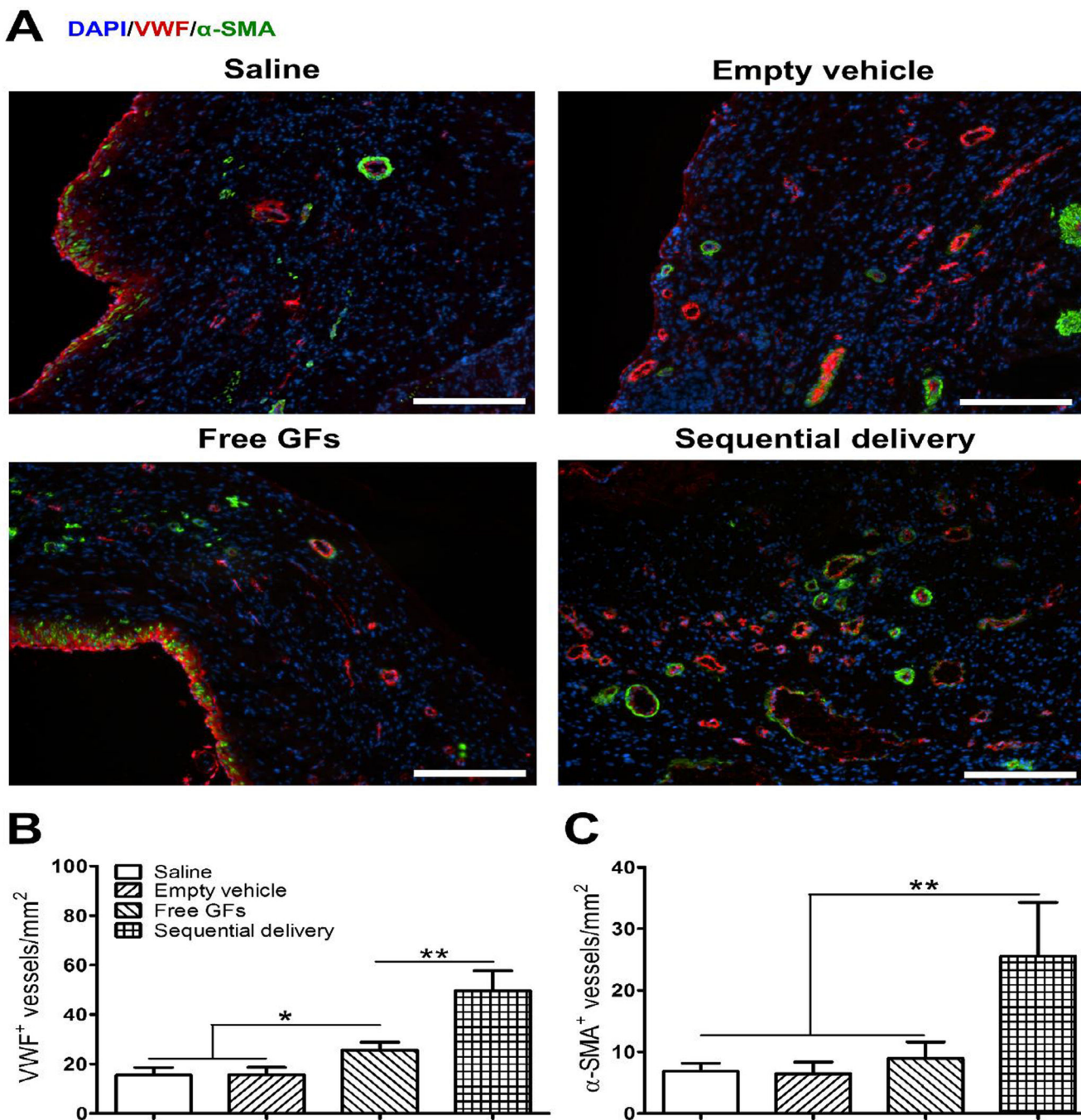


Fig. 6. Sequential delivery of VEGF and PDGF improves angiogenesis 4 wks after MI. (A) Representative images show co-staining of VWF (red) and α -SMA (green) that reflect the level of neovessel formation, their functionality and maturity, with noticeable improved angiogenesis in the sequential delivery group. (B) Saline and empty vehicle groups showed little angiogenesis with few VWF-positive vessels. While free GFs induced significantly more VWF-positive vessels than controls, sequential delivery induced significantly more than all groups. (C) Sequential delivery induced significantly more α -SMA-positive vessels

than all groups. Data are presented as means \pm SD (n=4–5 per group). * P <0.05, ** P <0.01.
Scale bar=200 μ m.

Author Manuscript

Author Manuscript

Author Manuscript

Author Manuscript

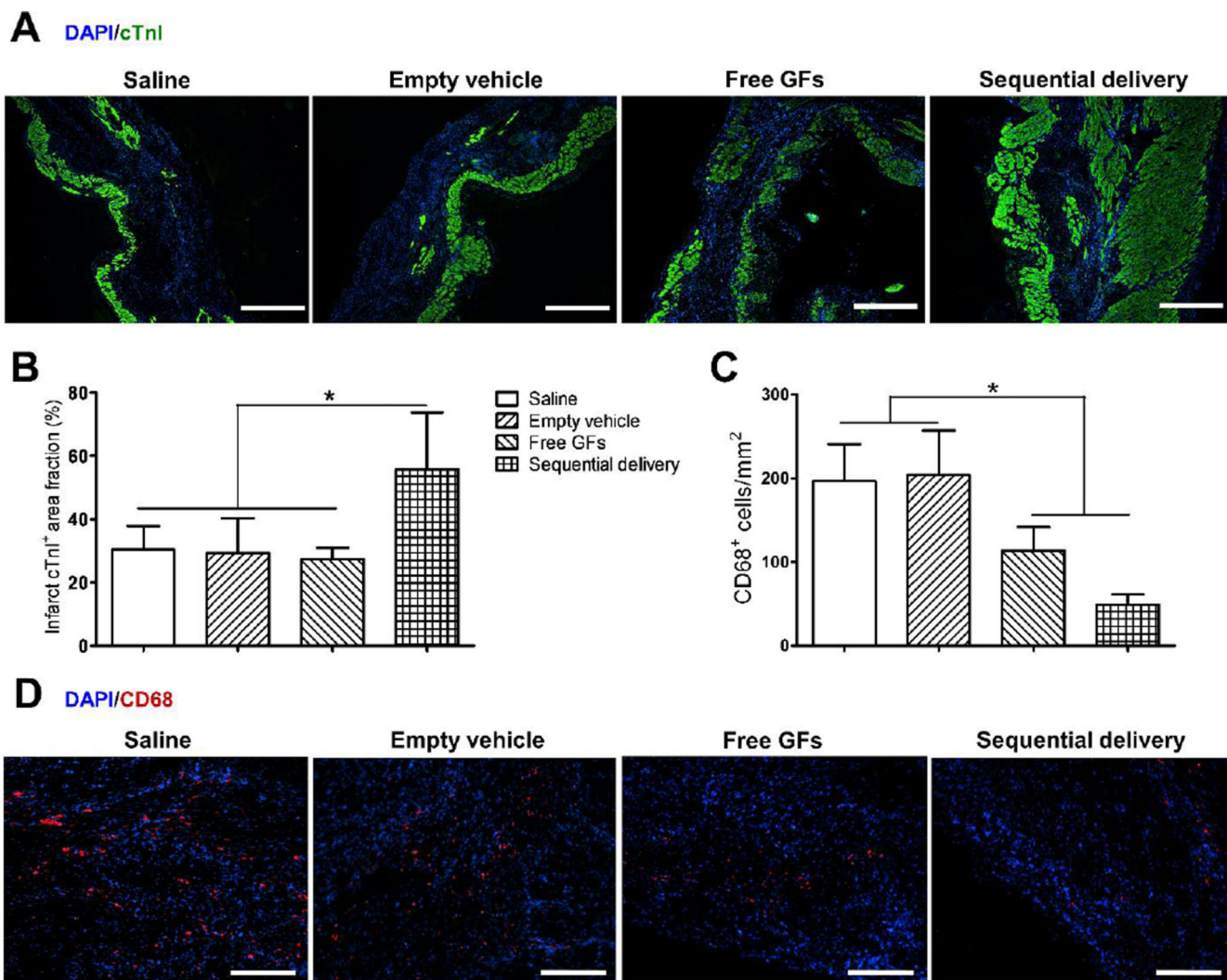


Fig. 7. Sequential delivery of VEGF and PDGF improves cardiac muscle viability and reduces inflammation 4 wks after MI. (A) Cardiac troponin I (cTnI) staining (green) showed few viable cardiomyocytes in saline, empty vehicle, and free GFs groups, while sequential delivery group showed a larger area of viable cardiac muscle in the infarct zone. Scale bar=500 μ m. (B) Quantitative analysis revealed that the sequential delivery group showed a significantly larger cTnI-positive area fraction in the infarct region compared to all groups. (C) Staining of inflammatory marker CD68 showed large numbers of CD68-positive cells in saline and empty vehicle groups, while significantly less cells were found in free GFs group and even less in sequential delivery group, with no significant difference between them. (D) Representative images of CD68 staining show less positive (red) cells in free GFs and sequential delivery groups. Scale bar=250 μ m. Data are presented as means \pm SD (n=4–5 per group). * P <0.05.